Precision alignment of the LIGO 4 km arms using the dual-frequency differential global positioning system

W. E. Althouse[1,2], S. D. Hand[3,4], L. K. Jones[1], A. Lazzarini[1], and R. Weiss[5]

[1]LIGO Laboratory at the California Institute of Technology, Pasadena, CA 91125
[2]Stanford Linear Accelerator Center, Menlo Park, CA 94025
[3]CB&I Services, Plainfield, Illinois 60606
[4]Jacobs Engineering, Livermore, CA 94550
[5]LIGO Laboratory at the Massacushetts Institute of Technology, Cambridge, MA 02139

The alignment of the Laser Interferometer Gravitational-wave Observatory (LIGO) using the Global Positioning System (GPS) is described. The LIGO project is designed to detect gravitational waves from astrophysical sources by laser interferometry. There are two sites separated by 3002 km that will be operated in coincidence. At each, site laser beams propagate in two orthogonal 4 km long evacuated beam lines 1.2 meters in diameter. The subject of this article is the alignment of the 16 km of beam tubes using dual-frequency differential GPS. A maximum deviation from straightness in inertial space of 5 mm rms and an orthogonality between arm pairs of better than 5 microradians is reported.

Analysis of the as-built alignment data allows a determination of the geodetic coordinates for the vertices and the arm orientations at both sites. From this information, the baseline distance between the vertices of the Hanford, WA and Livingston, LA sites has been determined to be 3001.8 km.

PACS numbers: 04.80.N, 06.20, 91.10Jf+Ws, 95.55.Y

I. Introduction

The Laser Interferometer Gravitational-wave Observatory (LIGO)[1,2,3] is dedicated to the direct measurement of gravitational waves from astrophysical sources. The project is funded by the National Science Foundation and is operated jointly by the California Institute of Technology (Caltech) and the Massachusetts Institute of Technology (MIT).

Gravitational waves are emitted by accelerating masses and are expected to be detectable at the Earth from sufficiently violent events occurring throughout the universe[4]. The formation and collision of black holes and the coalescence of orbiting compact stars, such as binary neutron stars or black holes, are likely sources. In addition, there is a possible residue from the primeval universal explosion. Einstein's Theory of General Relativity predicts that the waves travel at the speed of light and that they cause a distortion of spacetime transverse to their direction of propagation[5,6].

The direct detection of gravitational waves can provide fundamental evidence for the behavior of spacetime in strong gravitational fields where Newtonian gravitation is no longer a good approximation. Detection may also yield a new view of the universe since gravitational waves emerge from the densest regions in astrophysical processes without attenuation or scattering.

The LIGO facilities consist of two observatories, one located at the U.S. Department of Energy's Hanford Nuclear Reservation in Washington State (LIGO Hanford Observatory or LHO, see Figure 1.) and the other in Livingston Parish, Louisiana (LIGO Livingston Observatory or LLO). The site-to-site separation is 3002 km. This distance corresponds to a gravitational wave travel time of 10 ms. The interferometers located at the two sites are operated as a network. A network of detectors enables the determination of the position of sources on the sky from arrival time differences of the wave. It also reduces the influence of non-Gaussian environmental noise in the individual interferometers and thereby increases detection confidence.

LIGO detects the gravitational waves by comparing the time of propagation of light in mutually orthogonal paths in the distorted space between freely suspended test masses separated by 4 km using laser interferometry[7]. The distortions that need to be measured are not expected to be larger than a strain of 10^{-21}. The tubes, aligned by the GPS system described here, provide an evacuated and low scattering path for the laser beams (see Figure 2).

At the inception of the LIGO project construction, GPS surveying techniques had been applied to a number of large scale precision surveys[8,9,10] and the their use in construction had become a standard practice. LIGO, however, posed several unique challenges. The beam tubes needed to be aligned along the propagation direction of light in vacuum and not along the direction perpendicular to local gravity on the surface of the Earth[11]. The curvature of the Earth will cause the Earth's surface to deviate from the straight line propagated by light in vacuum by 1.25 meters over a 4 km path if the line starts out level with the surface. The alignment was, therefore, not the same as that for a level highway or pipeline. A second special consideration, dictated by the nature of the construction project, was that GPS alignment needed to be carried out concurrently with the construction with no significant opportunity for a check to be made by standard optical techniques until the construction was completed.

II. Method of alignment

LIGO contracted with CB&I Services, Inc. (CB&I) to design, fabricate, install and align the beam tubes. Proper alignment of the four four km beam tube sections was perceived as a major concern for LIGO. The beam lines require a minimum clear aperture of 1 m in order to accommodate multiple interferometers operating simultaneously within the same vacuum envelope. In addition, control of scattering and diffraction of light at an acceptable level for the most sensitive detectors contemplated in the facilities requires a large aperture. Refer to Figure 3.

The beam tubes are fabricated from 3 mm thick, spirally welded 304L stainless steel and have a nominal aperture diameter of 1.24 meters. 9 cm high optical baffles installed in the beam tube and fabrication and installation tolerances reduce the actual clear aperture to 1 m. These details are listed in Table 1 below. Construction of the beam tubes was undertaken in 2 km sections, called beam tube modules.

A. Feasibility studies and design

LIGO had identified in its 1989 conceptual design[12] the use of a high precision dual-frequency, differential Global Positioning System survey (GPS or DGPS) as a technique to set reference monuments that could be used as millimeter-level optical benchmarks. However, at the time of the proposal, GPS equipment and procedures to achieve this precision were not yet widely available to industry.

The introduction of commercially available, real time DGPS systems in 1993 permitted the use of GPS to be reconsidered by the time construction of the beam tube was to begin.

Trimble Navigation's Site Surveyor Real Time Kinematic (RTK) system was identified as an off-the-shelf system with millimeter-level accuracy that could perform in real time as needed in the field.

A field demonstration was performed to evaluate the capability of accurately measuring millimeter displacements using the dual frequency system. This test was performed by displacing a GPS receiver antenna vertically and horizontally with a translation stage and then comparing the GPS readout to a mechanical dial indicator. Accuracy and precision tests were performed with an integration time of 10 s. A total of ~260 points were measured for each of 3 displacement directions. Post-processing using a precise satellite ephemeris yielded 1σ (1-axis, horizontal) = 0.0009 m and 1σ (1-axis, vertical) = 0.0025 m (see Figure 4). The data also exhibited biases (i.e., non-zeroes means or offsets) in the distribution of residuals. The horizontal performance conforms very well to a normally distributed set of measurements. However, the vertical data exhibit a bimodality which, in the raw measurement-versus-actual displacement data sets, resembles a non-linearity for small vertical displacements. As a conservative estimate of overall measurement uncertainty, the root sum square (RSS) of measurement bias and variance was used for both axes. These results were used in the χ^2 analysis described later.

Similar repeatability tests were later conducted for each arm at both sites to confirm that no systematic effects were present. This also demonstrated that millimeter RMS precision was achievable along the 4 km arms.

The early field test results were incorporated in the final design of the beam tube. The nominal beam tube diameter was chosen as a trade-off among material costs, dimensional control of the fabrication process, and beam tube alignment accuracy. The trade study resulted in the allocation of errors presented in Table 1.

The beam tube supports were designed to incorporate a heavy stiffener with precision machined inside and outside surfaces to provide a center reference. By incorporating tight tolerances for concentricity of the stiffener rings, their outside diameter could be used as a reference to the beam tube centerline.

B. GPS equipment

CB&I chose Trimble Navigation’s Site Surveyor System for use on this project[13]. The following hardware configuration was used:

· GPS Dual Frequency Receivers 4000SSi with OTF and l MB Memory

- Data Collector TDC-1
- Geodetic Ground Plane Antennas
- TRIMTALK Radio System
- GPSurvey Software
- TRIMMAP Software
- Pacific Crest 35 W radio system in lieu of the V Systems
- 38 cm (15") Dorn-Margolan Choke Ring antennas to replace the Geodetic Ground Plane Antennas.

The 1MB RAM in the receiver was insufficient to accommodate a full day of acquired data at the 5 s integration and sampling rate that was used. The field technician was required to halt data acquisition and to download the fixed and roving receiver databases at 4-hour intervals. Incorporating a minimum of 3MB in the receiver would have greatly improved operational efficiency in the field.

C. Field implementation

1. Layout of the global coordinate system

The fundamental coordinate system for the alignment was the Earth ellipsoidal model WGS-84[14,15]. All raw GPS data were referred to this system using geodetic coordinates {height above ellipsoid [h], latitude [φ], longitude [λ]}. Geodetic coordinates were transformed to the standard earth-fixed Cartesian system $\{X_E, Y_E, Z_E\}$, where $\hat{z}_E$ is aligned along the earth's polar axis and $\hat{x}_E$ penetrates the ellipsoid at the intersection of the Greenwich Meridian with the Equator. $\hat{y}_E$ is perpendicular to both axes (refer to APPENDIX A).

A global coordinate system (denoted by a subscript "G") specific to each LIGO site was defined in which the $\hat{x}_G$ and $\hat{y}_G$ are aligned along the interferometer arms and $\hat{z}_G$ is normal to these axes. The interferometer plane was chosen to minimize construction costs (determined by the local topography) such that the global coordinate system lies in a plane that is locally tangent to the WGS-84 model at some point within the triangle defined by the 4 km arms. Deviations between local Zenith and $\hat{z}_G$ can range up to ~0.63×10^{-3} radian. The global coordinate systems for the two sites are further described in data analysis discussion in Section III.

The ends of the beam tube modules along each arm (i.e., at ~46 m, ~2012 m, ~2022 m, ~ 3989 m from the vertex) constituted controlled interface points. These points were identified by benchmarks (monuments) having measured geodetic coordinates that were provided by an independent surveyor. CB&I used these points together with an array of five other LIGO primary GPS monuments to calibrate their GPS instrumentation and software. The installation and survey of primary monuments was performed prior to beginning of the construction activities at the sites. At LHO the work was performed by the state Department of Transportation (WADOT) and it was performed by a private surveyor at LLO. The calibration was used by the GPS data acquisition system in real time to provide alignment data in global coordinates.

Using global coordinates, the beam tube centerlines were marked along the foundation slab at points spaced uniformly at ~20 m intervals (the unit length of beam tube sections that were welded together in the field) along both arms.

A straight line in space varies in ellipsoidal height by ~1.25 m over a 4 km baseline. At each of the fiducial points, the design ellipsoidal height of the beam tube centerline was calculated using the WGS-84 model with the latitude and longitude as inputs. These heights were used to perform preliminary alignment of the tube sections as the supports were installed during beam tube fabrication on the slab.

Fiducial points were surveyed using a layout cart (refer to Figure 5). The cart was equipped with linear bearings and a plumb alignment bracket and modified to support a fixed height antenna rod. Antenna rods, levels and attachment fixtures were periodically calibrated to better than 0.25 mm accuracy to ensure repeatability of measurements. Antenna rods used a leveling device consisting of a coincidence-type bubble level with a sensitivity of 10 arcsec/mm. This arrangement provided acceptable repeatability in a reasonable set-up time. After a nominal fiducial point was identified, a 15 - 20 minute static control point measurement was taken to provide a location determination. The nominal fiducial point was adjusted if required and a scribed mark was made on the foundation slab for the tube installation crew to use for rough elevation and centering of the tube section and its support.

2. Final Alignment

At Hanford, supports were aligned for the final time after installation had proceeded 3 - 4 sections, i.e. ~80 m from the installation activity. This was just before the beam tube became covered by cement enclosures and was thus no longer directly available. At Livingston, the beam tube enclosure sections were core drilled directly over the beam

tube supports at ~120 m intervals. This design improvement allowed alignment to be confirmed after fabrication was completed.

The final alignment fixtures were similar for both sites (refer to Figure 6). The antenna rod was longer in Livingston to enable the antenna to protrude through the cored enclosure. The fixture was a high accuracy centering head clamped on the machined beam tube support stiffener ring, plumbed using a coincidence level and centered relative to the beam tube support stiffening ring. The GPS antenna[16] was attached to a rod of calibrated length. The reference distance from the beam tube centerline to the antenna was taken as the rod length plus the radius of the beam tube support stiffener.

With this fixture in place, the GPS receiver was set to the Real Time Kinematic (RTK) "stake-out" mode to position the beam tube center to the desired position relative to the global coordinate system. Once the position was determined to be within a few mm of the desired location, the support was locked down. A 30 minute control point measurement was then taken and the raw data were logged by the receiver for subsequent post processing. The control measurement was taken in the RTK mode to verify position and to allow real-time adjustment. Whenever an adjustment was required, a repeat 30 minute control measurement was taken to verify the change.

3. GPS reference points outside enclosures

Additional GPS reference points were located (only at LHO) outside the beam tube covers to provide the ability to monitor the foundation slab for long-term height changes from settlement. These reference points were placed at the edge of the foundation slab in line with each support ring. A two axis centering tripod designed to hold and adjust a fixed length GPS antenna rod was used (refer to Figure 7). A 30 minute static control point measurement was taken for each point. In addition, a cross-check was made using Trimble’s RTK stake-out procedure. These data serve as a reference for future GPS surveys that are made to assess slab settlement.

4. Post processing and data review in the field

Data quality review was incorporated as part of the daily field alignment procedure. Precise GPS satellite ephemeris data were employed to determine post-processed positions. The ephemeris data were downloaded from the US Coast Guard web site [17].

Satellite residuals for each data point were determined relative to the reference mean for that point. Residuals were evaluated for consistency with the mean to identify and

eliminate outliers. For every point surveyed, the time dependence of residuals from all visible satellites were displayed graphically. Typically, outliers arise from data coming from satellites lying closest to the local horizon. Residuals exhibiting non-statistical fluctuations were eliminated by moving the satellite elevation cutoff to higher zenith angles or by eliminating data from suspect satellites. There is a trade-off between degradation of signal-to-noise ratio (SNR), which decreases as satellites are removed from the analysis, and better data repeatability, which improves as data from marginally visible satellites are removed. After post processing, CB&I determined the geodetic coordinates of all points measured along the beam tubes. These were provided to LIGO for further analysis.

III. Definition of global coordinate systems and analysis of beam tube alignment data

The final alignment data provided by CB&I were analyzed by LIGO to determine the residuals relative to the best-fit descriptions for each site of the local right-handed coordinate systems that have their X and Y axes aligned along the beam tube arms. The methods employed at each site differed and reflected the accrued experience. These are described below.

A. Hanford, Washington

1. Definition of the global coordinate axes

The interface benchmarks that are located at the termini and midpoints of each arm were used in a non-linear regression analysis to first determine the best-fit description for the global coordinate axes. The data consisted of repeated measurements by independent surveying contractors for each of the 8 positions located at nominally {46 m, 2012 m, 2022 m, 3989 m} along the two arms. The data were used in a χ^2 minimization of the transverse (2D) residuals of the benchmark positions to determine the best-fit axes. There are six degrees of freedom for the fit: 3 translational and 3 rotational. These were chosen as follows:

- **three** coordinates for the vertex, $\{X_v, Y_v, Z_v\}$;
- **two** vector components for the $\hat{x}_G$ axis, $\{n_{xx}, n_{xy}, 1\}$; the n_{xz} component was kept fixed. The unit vector was obtained by normalization in a second step.
- **one** vector component for the $\hat{y}_G$ axis, $\{n_{yx}, -(1+n_{xx}n_{yx})/n_{xy}, 1\}$; the orientation of the Y axis was constrained to lie in the plane normal to the X axis. This is achieved by

varying only the x component of the Y axis direction, constraining its y and z components. The unit vector was obtained by normalization in a second step.

Not all errors associated with the measured data points were reported in the surveys. Therefore we used the measurement statistics that were shown Figure 4 for all data points.

The RMS residual of the input data with respect to the best fit axes was 0.005 m with a χ^2 statistic of 1.5 per DOF for 75 DOFs. This fit yields the parameters listed in Table 2.

2. Results for the as-built beam tube arms at Hanford

The geodetic coordinates for the beam tube center positions reported by CB&I were converted to earth-fixed Cartesian coordinates using the relationships described in APPENDIX A. The points were transformed into the global coordinate system of Table 2. The values for δY_G and δZ_G along the X-arm (or δX_G and δZ_G along the Y-arm) are the residual alignment errors for each beam tube support position, and include both measurement errors and actual positioning errors.

Figure 8a presents the residuals in the transverse directions as a function of axial position along the beam tube arms. Some periodic and systematic trends are evident; however the magnitudes of the residuals meet LIGO specifications. A small amount of skewness (~0.004 m, see Figure 9) is evident between the arms (i.e., the lines which best described the two arms individually do not intersect). The X arm was the first to be aligned and exhibits more scatter in the data. The better statistical characteristics of the Y arm are due to the improved alignment techniques that evolved with increasing experience in the field. Figure 9a, b are scatter plots of the GPS measurements for both arms at Hanford. These are the same data as in Figure 8a, viewed along the global coordinate system X or Y axes

Both beam tubes at Hanford are aligned to their respective axes to better than 0.005 m RMS (2-axis). This quality of alignment comfortably meets LIGO requirements. Table 3 presents the means and standard deviations for the transverse dimensions along both arms. These results comprise a total of 404 data points taken at 20 m intervals and distributed equally between the arms.

After beam tube alignment by CB&I, LIGO employed the services of a surveying company (Rogers Surveying, Inc., or RSI) to verify the GPS based alignment data by independent means. Quality checks of the CB&I data were performed for a large number

of selected points along both arms. The checks were performed for both vertical and horizontal alignment by using a combination of optical and gravimetric techniques. We present data only for the vertical alignment verification because this dimension is the one for which GPS accuracies are worse typically by a factor ~3X. We note that the horizontal alignment data in the lower panels of Figure 8a exhibit less variability and less evidence of systematics, which reflects the fact that horizontal positional accuracies are generally better with GPS.

The follow-up surveys provided orthometric heights relative to the geoid (as opposed to the ellipsoidal heights provided by GPS). The geoidal deviations from the WGS-84 at each of the measurement points were calculated with a software package from the U. S. National Geodetic Survey using the GEOID96 model[18]. The orthometric height data provided by RSI were presented as differential data for each arm separately (differences of heights as one proceeds along each arm). In order to obtain absolute data connecting both arms, a choice of reference datum was required. Two different datums were selected: (i) the first interface point along the X arm at X_G = 46 m as determined by RSI and (ii) the same datum as determined earlier by a third independent surveyor, IMTEC. These cross checks are presented in the top two graphs in Figure 8a.

The RSI reference data are denoted as *Cross-check 1* and *Cross-check 2* and are indicated by '×' and 'Δ' in the plots. The overall concordance between CB&I's reported alignment data and the quality checks is evident and meets LIGO requirements. This established confidence in CB&I's quality of data so that subsequently fewer cross-checks were deemed necessary.

B. Livingston, Louisiana

The alignment of the Livingston beam tube arms proceeded in a different manner from what was done at Hanford. Experience with the quality of alignment at Hanford led to the decision to use CB&I's alignment database as the primary basis for determining the global coordinate system without relying on independent surveys. Hence, instead of using only 8 interface points to determine the global coordinate system, all available alignment data were used.

CB&I core-drilled the beam tube enclosures and developed a direct in-situ final alignment procedure with a contacting fixture at 64 control points where GPS measurements were made directly on the as-built beam tubes. We used the interface points in defining the module ends, just as at LHO, and the rest of the module was defined as being in a straight line between those points. The core-drilled control points

were used as a final check of alignment. We used the measurement statistics that were described earlier for all data points.

The RMS residual for the best fit was 0.004 m with a χ^2 statistic of 1.9 per DOF for 186 DOFs. Table 4 presents the parameters describing the best-fit coordinate axes in Livingston.

The 404 alignment data points reported by CB&I for every 20 m along the beam tubes were transformed to global coordinates in the same manner described for Hanford. Both beam tubes at Livingston are straight to better than 0.004 m RMS (2-axis). This quality of alignment comfortably meets LIGO requirements. Table 3 presents the means and standard deviations for the two transverse dimensions along each arm.

Figure 8b presents the residuals in the transverse directions as a function of axial position along the beam tube arms. Systematic trends in the horizontal error with axial position are evident. This indicates that the beam tube centerlines are slightly non-orthogonal. In fact, the lines which best describe the centerlines subtend an included angle which is greater than 90° by 5.3 microradians. The small non-orthogonality of the arms resulted from the initial benchmark data provided by LIGO to CB&I: subsequent analysis of the larger data set revealed the deviation. If we remove the linear trend from the residuals that is caused by this slight non-orthogonality, then the best-fit (but non-orthogonal) centerlines result in RMS residuals of 0.002 m (X arm) and 0.001 m (Y arm). Aside from the (acceptably small) non- orthogonality of the arms, the quality of alignment is better than it was at Hanford: once again, the accrued experience and improved procedures of the CB&I team are evident.

Figure 9c, d show scatter plots of the GPS measurements for both arms at Livingston. There is no evidence of skewness for the Livingston site.

IV. Discussion

The data acquisition techniques described above were developed by a CB&I senior field engineer and were successfully transferred to skilled technicians who then executed them repeatedly with consistent results. The sub-centimeter levels of precision achieved demonstrate the utility of DGPS for *routine* applications in the field. By using the procedures described above the effort needed to align large-scale systems such as LIGO was significantly less than it would have been had we relied on conventional techniques.

The layout of the beam tubes and the orientations determined by GPS in the manner described were subsequently used to erect survey monuments to align the laser beams down each arm by dead reckoning. The monuments were erected in the vicinity of the vertex at each site and the directions to the 2 km and 4 km distant mirrors were defined. In defining these directions, only the first few hundred meters of the arms could be used due to practical constraints. Thus the angular pointing accuracy expected in deriving the directions to the distant mirrors was of order $\sigma_\theta \sim \sigma_x/200\text{m} \sim 25 \times 10^{-6}$ radian.

The laser beams have been propagated down the evacuated 2 km beam tube module at Hanford and the full 4 km long arm at Livingston. The beam pointing derived from the survey markers resulted in a dead reckoning alignment of the beams to approximately 50 microradians. This angular uncertainty is consistent with expectation. However, it does correspond to a transverse error of 20 cm at the end of a 4 km path and this does not approach the alignment precision of 5 mm determined from the GPS alignment. Nevertheless, it was extremely satisfying to see the beam and established that there were no large systematic errors though the random errors were known to be small. The direct measurement of the alignment using the laser beams will be improved as the LIGO interferometers are commissioned and this will provide a more stringent comparison of the GPS and optical alignment.

V. Acknowledgements

The authors gratefully acknowledge Professor Thomas Herring of the MIT Department of Earth, Atmospheric and Planetary Sciences. He provided valuable insights into the field use of GPS surveying equipment during the early phases of the project. He suggested using absorbing sheet (ECCOSORB[19]) at the ground plane of the receiving antenna in order to improve the SNR during field measurements. He also provided CB&I with a computer program to calculate the ellipsoidal conversion.

One of the authors (S. H.) also wishes to acknowledge Mr. Dennis E. Dickinson, of CB&I, who worked in the field to acquire GPS data at both sites and who managed the final inspections and field reduction of the GPS data for the Livingston, LA beam tubes. Mr. Hugh L. Johnston, of Trimble Navigation provided the initial concepts for adapting RTK GPS techniques to provide the high accuracy needed by LIGO. Finally, Mr. Randy E. Melton, of GPS Innovations, Charleston, WV provided training and insight to the operation of GPS equipment and software.

The LIGO Project and LIGO Laboratory are supported by the National Science Foundation under cooperative agreement PHY-9210038. This paper has been assigned LIGO Document Number LIGO-P000006-C-E.

APPENDIX A

The Earth-fixed Cartesian system $\{\hat{x}_E, \hat{y}_E, \hat{z}_E\}$ is used for geodetic work. In this system, $\hat{x}_E$ pierces the earth surface at {φ,λ} = {000, 000}, $\hat{y}_E$ pierces the earth's surface at {φ,λ} = {000, 090E}, and $\hat{z}_E$ pierces the earth's surface at φ = 090N. The relationship between the coordinates of a point {h, φ, λ} and $\{X_E, Y_E, Z_E\}$ is depicted graphically in Figure 10.

The functional relationships are given by:

$$X_E = (R[\phi] + h)Cos\phi Cos\lambda$$

$$Y_E = (R[\phi] + h)Cos\phi Sin\lambda$$

$$Z_E = ((1 - \varepsilon^2)R[\phi] + h)Sin\phi$$

The earth model WGS-84, is described by an oblate ellipsoid with its semi-minor axis, b = 6356752.314 m, along $\hat{z}_E$, semi-major axis with value a = 6378137 m, and eccentricity given by $(1 - \varepsilon^2) = 0.993306$. R[φ] is the local radius of curvature of the ellipsoid at latitude φ:

$$R[\phi] = \frac{a^2}{\sqrt{a^2 Cos^2\phi + b^2 Sin^2\phi}}$$

Note that in the geodetic model the vector h is aligned along the local surface normal. Consequently, its extension to the equatorial plane will not in general intersect the origin.

Table 1: Allocation of budgeted tolerances for the beam tube clear aperture

Description	Value[a] (m)
Fabricated beam tube aperture, minimum	1.238
Optical baffling system[b]	0.202
Sources of aperture degradation during fabrication and installation	
Straightness[c]	0.010
Concentricity errors	0.010
Ellipticity of beam tube cross section	0.006
GPS measurement error and tube placement tolerance	0.018
Net clear aperture	0.992

a. Errors are given as peak-to-peak values on the diameter and are added algebraically to compute total allowed error.

b. To control stray scattered light, the beam tubes are lined with strategically placed sheet metal baffles which protrude radially into the beam tube by 0.090 m. Tolerances on the design result in an allotment of 0.101 m for the total radial projection.

c. Includes "corkscrewing" due to fabrication (0.006 m), thermal warping and sagging due to weight of the tube material (0.004 m).

Table 2: Parameters of the global coordinate system for Hanford, WA

Parameter	Value	Estimated Error	Units
Vertex	Geodetic {h,φ,λ}: {142.555,{N46°27'18.527841"},{W119°24'27.565681"}} Earth-fixed {X_E, Y_E, Z_E}: {-2.161414928×10^6, -3.834695183×10^6, 4.600350224×10^6}	- {0.006, 0.006, 0.005}[a]	{m, {dms}, {dms}} m
$\hat{x}_G$	Earth-fixed { $\hat{x}_E$, $\hat{y}_E$, $\hat{z}_E$ }: {-0.223891216, 0.799830697, 0.556905359}	-	
	Compass Direction: N35.9993°W (ref. geodetic north)[b]	2×10^{-6}	radian
	Angle below local horizontal at Vertex: 6.196×10^{-4}	3×10^{-6}	radian
$\hat{y}_G$	Earth-fixed { $\hat{x}_E$, $\hat{y}_E$, $\hat{z}_E$ }: {-0.913978490, 0.0260953206, -0.404922650}	-	
	Compass Direction: S54.0007°W (see footnote b)	2×10^{-6}	radian
	Angle above local horizontal at Vertex: 1.24×10^{-5}	3×10^{-6}	radian
$\hat{z}_G$	Earth-fixed { $\hat{x}_E$, $\hat{y}_E$, $\hat{z}_E$ }: {-0.338402190,-0.599658144, 0.725185541}		
	Deviation from zenith at vertex: 6.195×10^{-4}, toward $\hat{x}_G$	3×10^{-6}	radian

a With respect to the physical location of the benchmarks.

b. Site drawings call for the arms to run N36.8°W and S53.2°W; these are referenced to the WA State Plane Lambert South Zone NAD 83/91. Geodetic North is 47'39" (~ 0.8°) W of grid north at the vertex.

Table 3: Statistical description of the residuals for both sites.

Quantity	Mean, μ	Std. Dev., σ
Hanford, WA		
X arm, δZ	0.0007 m	0.003 m
X arm, δY	0.00006 m	0.003 m
Y arm, δZ	0.005 m	0.002 m
Y arm, δX	0.0003 m	0.002 m
Livingston, LA		
X arm, δZ	0.0002 m	0.002 m
X arm, δY	-0.0006 m	0.003 m
Y arm, δZ	0.002 m	0.002 m
Y arm, δX	-0.0008 m	0.003 m

Table 4: Parameters of the global coordinate system for Livingston, LA

Parameter	Value	Estimated Error	Units
Vertex	Geodetic {h,φ,λ}: {-6.574, {N30°33'46.419531"}, {W90°46'27.265294"}} Earth-fixed $\{X_E, Y_E, Z_E\}$: $\{-74276.04192, -5.496283721 \times 10^6, 3.224257016 \times 10^6\}$	- {0.006, 0.006, 0.004}[a]	{m, {dms}, {dms}} m
$\hat{x}_G$	Earth-fixed $\{\hat{x}_E, \hat{y}_E, \hat{z}_E\}$: {-0.954574615, -0.141579994, -0..262187738}	-	
	Compass Direction: S72.2836°W (ref. geodetic north)[b]	2×10^{-6}	radian
	Angle below local horizontal at Vertex: 3.121×10^{-4}	2×10^{-6}	radian
$\hat{y}_G$	Earth-fixed $\{\hat{x}_E, \hat{y}_E, \hat{z}_E\}$: {0.297740169,-0.487910627,-0.820544948}	-	
	Compass Direction: S17.7164°E (see footnote b)	2×10^{-6}	radian
	Angle below local horizontal at Vertex: 6.107×10^{-4}	2×10^{-6}	radian
$\hat{z}_G$	Earth-fixed $\{\hat{x}_E, \hat{y}_E, \hat{z}_E\}$: {-0.011751435,-0.861335199,0.507901150}		
	Deviation from zenith at vertex: 3.121×10^{-4}, toward $\hat{x}_G$ 6.107×10^{-4}, toward $\hat{y}_G$	2×10^{-6}	radian

a With respect to the physical location of the benchmarks.

b. Site drawings call for the arms to run S72°W and S18°E; these are referenced to Lambert Grid coordinates, NAD 83/92, Louisiana South Zone (1702). Geodetic North is 17'01" (~ 0.28°) W of grid north at the vertex.

LIST OF FIGURES

Figure 10: Schematic showing the relationship between Geodetic and Earth-Fixed Coordinate Systems.

LIST OF REFERENCES

[1] Abramovici, A. *et al.* Science **256**, 325 (1992).

[2] Barish, B.C. and Weiss, R. Phys. Today, **52**, 44 (1999)

[3] http://www.ligo.caltech.edu/

[4] Thorne, K.S., in 300 Years of Gravitation, edited by S. Hawking and W. Israel, (Cambridge University, Cambridge, 1987) Ch. 9.

[5] Einstein, A., "Naherungsweise Integration der Feldgleichingen der Gravitation," Sitzungberichte der Koeniglichen Preusissichen Akandemie der Wissenschaften, Sitzung der physikalish-mathematischen Klasse, p. 688 (1916).

[6] Einstein, A., "Ueber Gravitationswellen," Sitzungberichte der Koeniglichen Preusissichen Akandemie der Wissenschaften, Sitzung der physikalish-mathematischen Klasse, p. 154 (1918).

[7] Saulson, P.R., Fundamentals of Interferometric Gravitational Wave Detectors (World Scientific, Singapore, 1994).

[8] Collins, J. and Leick, A., 1st International Symposium on Precision Positioning with GPS, Vol. **2**, 667 (1985).

[9] Ruland, R. and Leick, A., 1st International Symposium on Precision Positioning with GPS, Vol. **1**, 483 (1985).

[10] Leick, A., Aiken, C., and Kor. J., Surveying and Land Information Systems, Vol. **52** No. 2, 69 (1992).

[11]The deflection of light in a 4km path on the Earth's surface due to the gravitational field of the Earth is less than 2×10^{-9} m.

[12] "A Laser Interferometer Gravitational-Wave Observatory (LIGO)", Proposal to the National Science Foundation, December 1989.

[13] CB&I, as the contractor, had sole responsibility for the choice of hardware for the project. This information is provided for technical communication purposes only and does not constitute an endorsement by either the National Scientce Foundation or the California Institute of Technology.

[14] B. Hoffman-Wellenhog, H. Lichtenegger, and J. Collins, GPS Theory and Practice, 3rd Ed., (Springer-Verlag, Wien, New York, 1994).

[15] A. Leick, GPS Satellite Surveying, 2nd Ed., (J. Wiley & Sons, New York, 1995).

[16] One source of systematic error is multi-path interference. LIGO's geometry and conducting beam tubes posed a concern. To eliminate this source of error, a 61 cm × 61 cm square of "ECHOSORB" material was placed a distance 0.095 m ($\lambda_{L1}/2$) beneath the GPS antenna. This material served to define the GPS antenna's field of view to include only the upper hemisphere viewing the sky. This improved SNR from 10% to 25%.

[17] http://www.navcen.uscg.mil/GPS/precise/

[18] http://www.ngs.noaa.gov/GEOID/geoid.html
http://www.cs.umt.edu/GEOLOGY/classes/Enviro_Geophys/geoid96.html

[19] ECHOSORB is a registered trademark of the Emerson Cummings Company, http://www.eccosorb.com

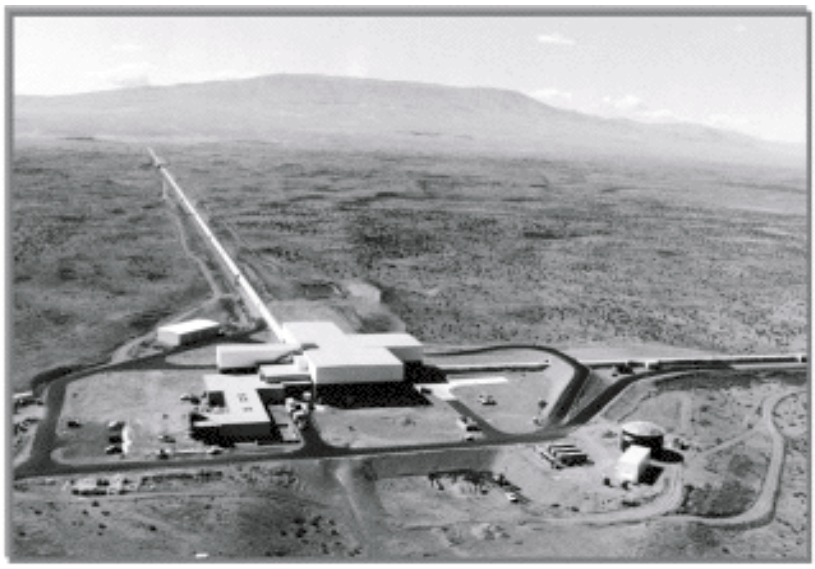

Figure 1
Althouse, Hand, Jones, Lazzarini & Weiss

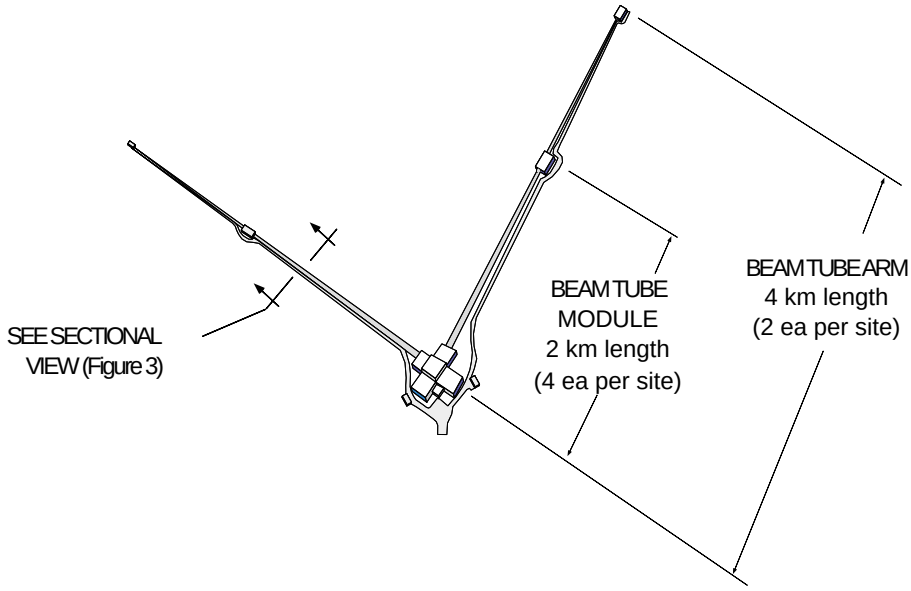

Figure 2
Althouse, Hand, Jones, Lazzarini & Weiss

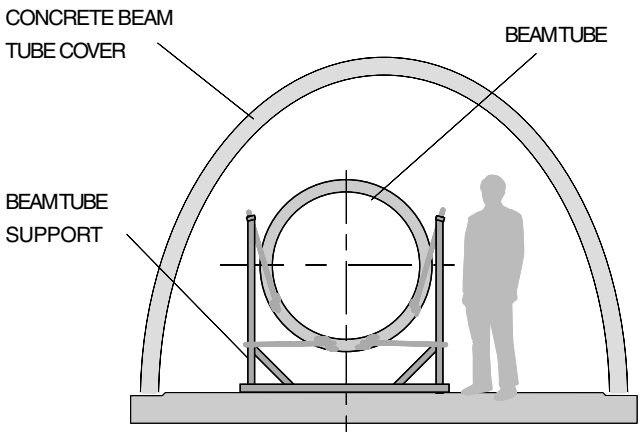

Figure 3
Althouse, Hand, Jones, Lazzarini & Weiss

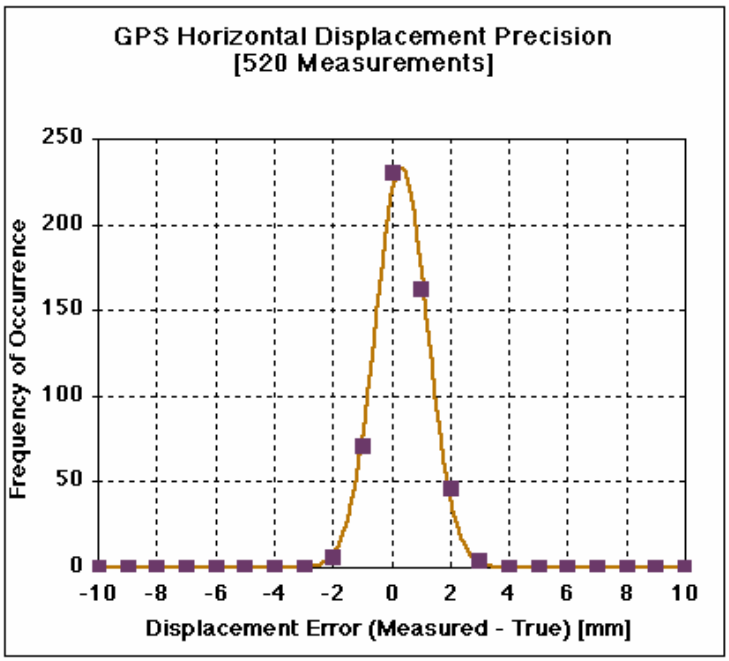

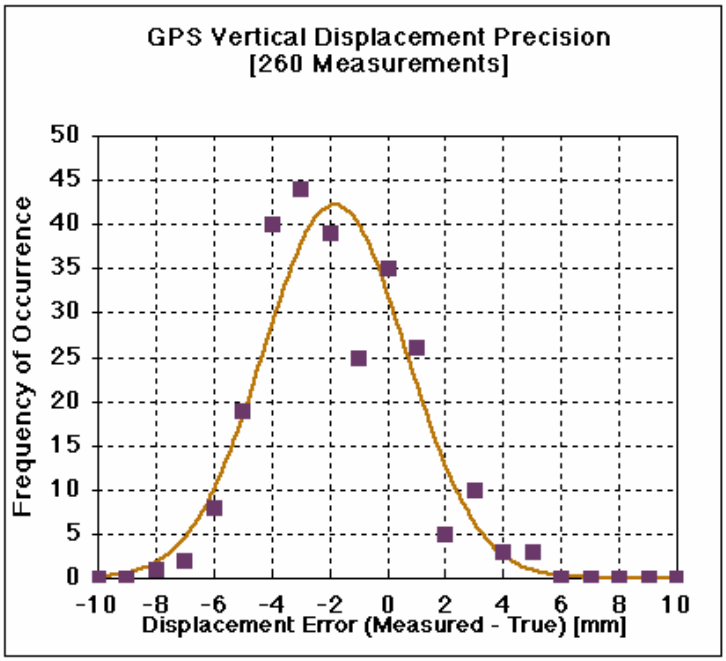

Figure 4
Althouse, Hand, Jones, Lazzarini & Weiss

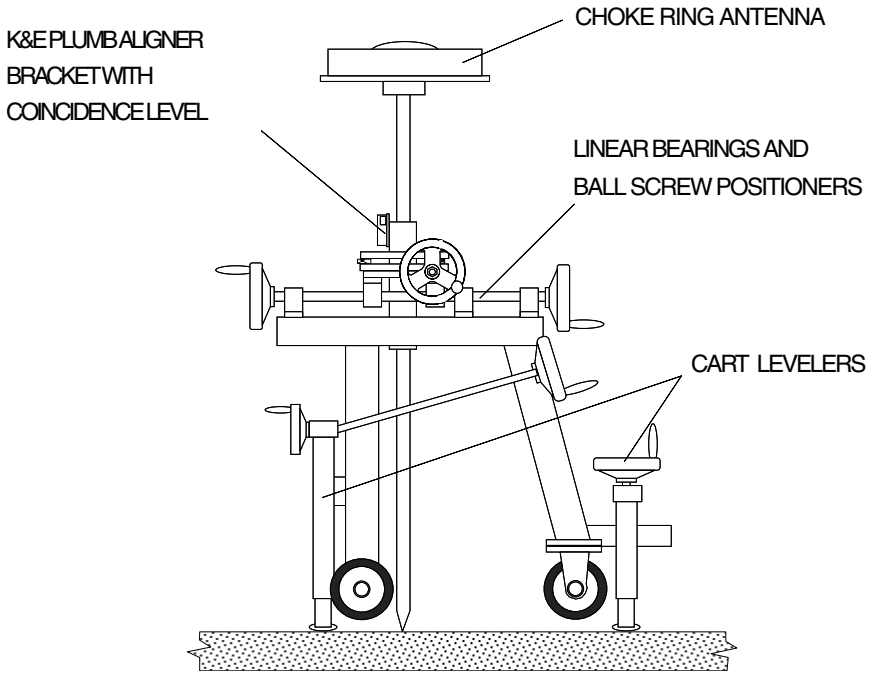

Figure 5
Althouse, Hand, Jones, Lazzarini & Weiss

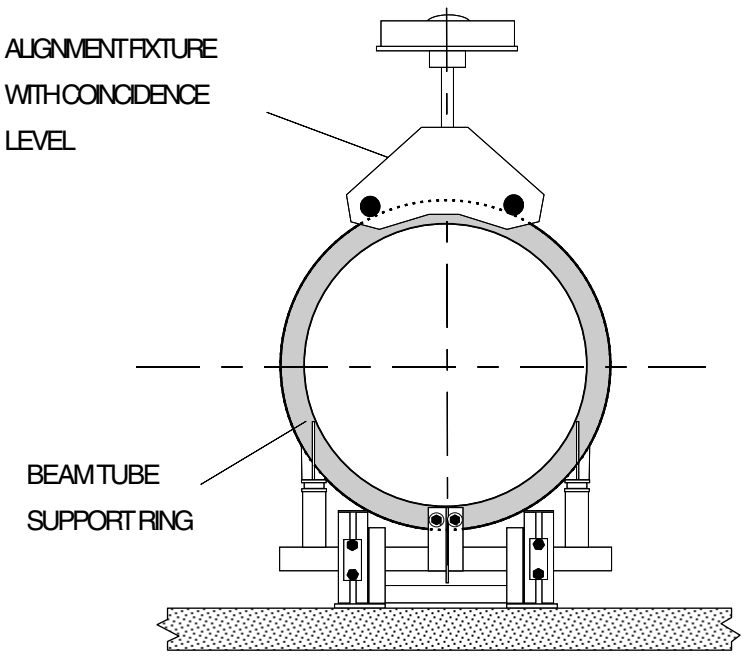

Figure 6
Althouse, Hand, Jones, Lazzarini & Weiss

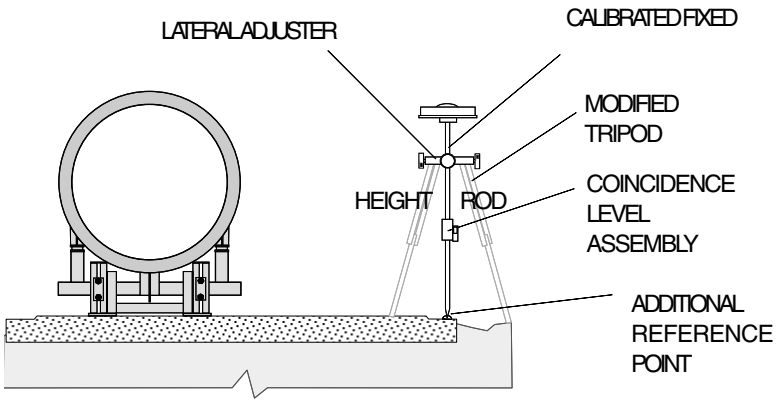

Figure 7
Althouse, Hand, Jones, Lazzarini & Weiss

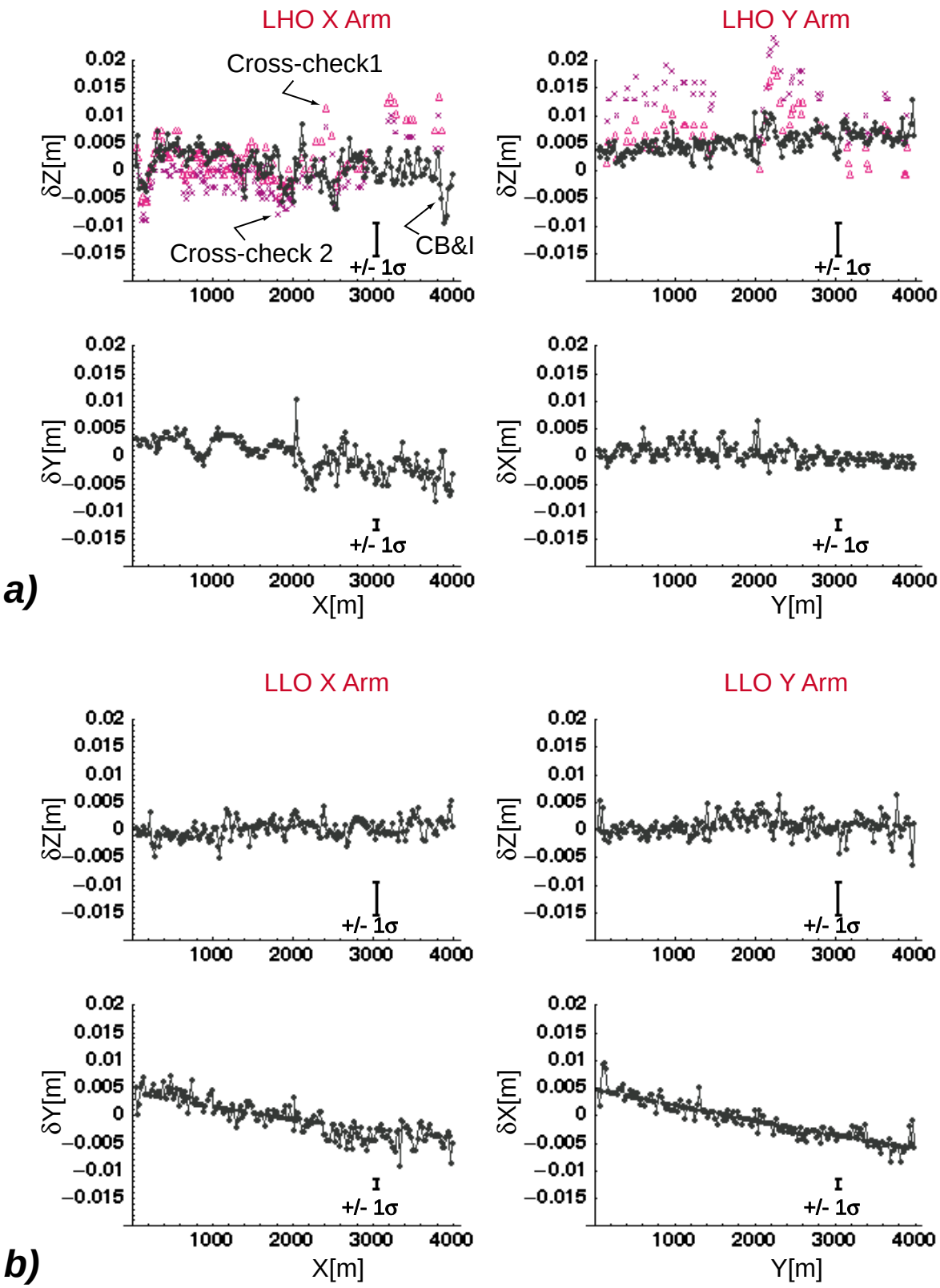

Figure 8
Althouse, Hand, Jones, Lazzarini & Weiss

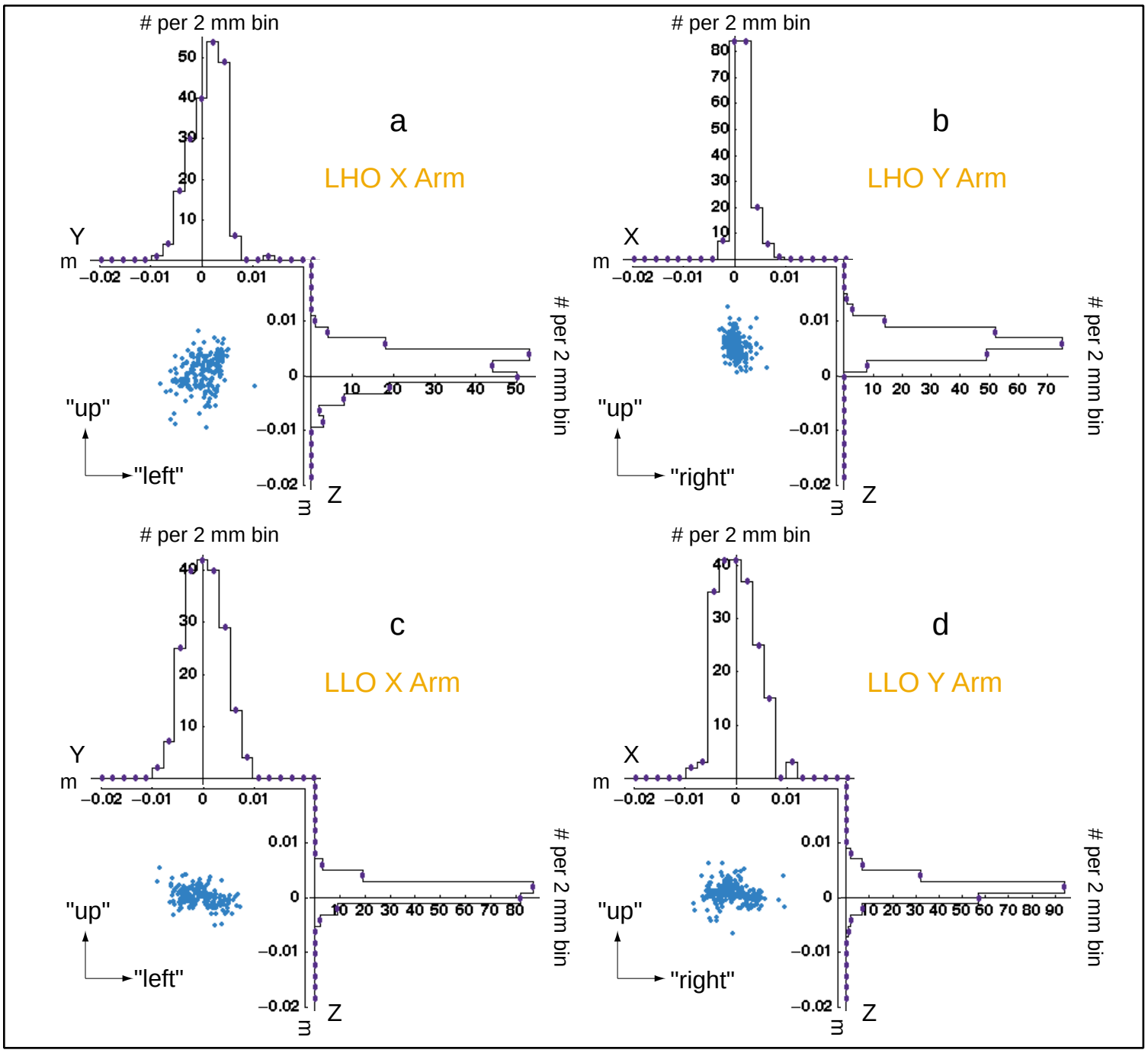

Figure 9
Althouse, Hand, Jones, Lazzarini & Weiss

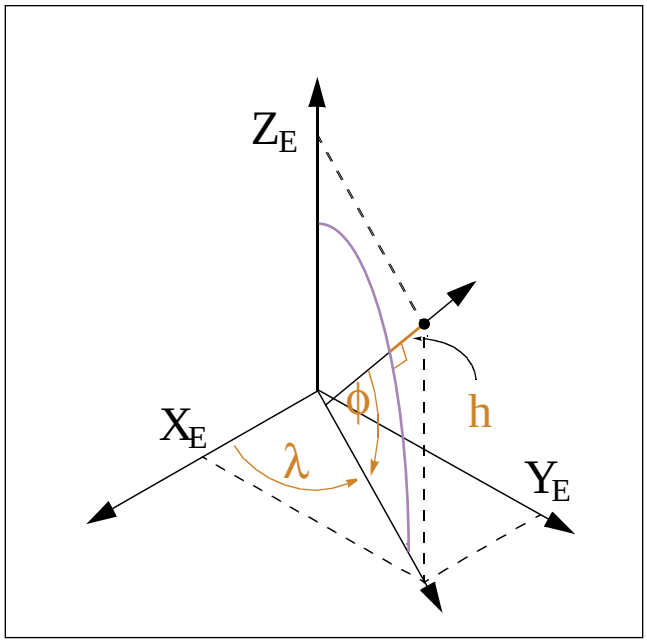

Figure 10
Althouse, Hand, Jones, Lazzarini & Weiss